Article citation info:
Puzdrowska P, Skobyłko K. Analysis of the possibility of using the Sankey diagram in the diagnosis of a partially loaded diesel engine. Combustion Engines. 2025;202(3):58-66. https://doi.org/10.19206/CE-205607

Patrycja PUZDROWSKA
Jakub SKOBYŁKO

Combustion Engines
Polish Scientific Society of Combustion Engines

Analysis of the possibility of using the Sankey diagram in the diagnosis of a partially loaded diesel engine

ARTICLE INFO

Received: 15 April 2025
Revised: 23 May 2025
Accepted: 27 May 2025
Available online: 13 June 2025

The purpose of this article is to determine if, in the case of inability to carry out diagnostic tests at engine operating loads in the range of 70–90%, engine functional systems can generate diagnostic signals in the form of changes in heat balance components. The motivation for working on the selected topic was the need to evaluate the effectiveness of graphical forms of heat balance representation, especially Sankey diagrams, in heat engine diagnostics, using a four-stroke diesel engine as an example. Interpretation of the results was carried out based on simulations performed using Blitz-PRO software and experimental tests carried out on a test bench. For the numerical simulations, the object under analysis was modeled, which was a single-cylinder, four-stroke diesel engine Andoria S320. Both numerical simulations and experimental tests were carried out for three engine operating states: the reference state and two malfunction states: in the air intake system and the fuel supply system. The analyses made it possible to draw conclusions. It was assessed that carrying out the analysis of the Sankey diagram for partial load doesn't bring significant diagnostic information.

Key words: *compression ignition engine, parametric diagnostics, Sankey diagram, numerical simulations, Blitz-PRO program*

1. Introduction

Maintaining stable operating parameters of a diesel engine and performing regular diagnostics is important, as it allows for the prevention of damage and degradation of entire functional systems and to operate the engine economically [7]. In IC engines, the most frequently diagnosed defects include the fuel supply system and the intake air system [3, 5]. Injector spring relaxation is indicated as one of the common failures of the fuel supply system. The consequence of this malfunction is incomplete combustion of fuel, which negatively affects the efficiency of engine operation. In turn, considering the air intake system, filter contamination can be a significant problem, restricting the free flow of air, thus reducing the efficiency of the engine's working processes [3, 12].

One of the diagnostic methods used in the analysis of IC engines is the evaluation of heat balances. Significant deviations from reference values, characteristic of a fully operational engine, can help indicate the functional system in which the malfunction has occurred [15]. Graphical tools such as Sankey charts are particularly useful for clearly interpreting the data obtained [4, 8, 11].

The purpose of the research presented in this article was to assess whether, under limited engine load conditions (less than 50%), engine functional systems generate diagnostic signals in the form of changes in heat balance components. The article presents some of the results obtained during the completion of the master's thesis for the energy technology faculty [13].

2. Description of the considered diagnostic method – Sankey's diagram

A diagnostic method based on the Sankey diagram involves graphically representing the flow of energy or mass within the system using a flow diagram [7]. In the case of a IC engine, the Sankey diagram illustrates the distribution of input energy $\dot{Q}_{fuel} + \dot{H}_{air}$ (energy contained in the fuel-air mixture) into several branches: indicated power P_i which can be separated into mechanical power Pm and effective power Pe), heat loss through exhaust gases $\dot{H}_{exh}$, s losses in lubricating oil $\dot{Q}_{oil}$, and cooling system $\dot{Q}_{cool}$, heat transferred to the environment $\dot{Q}_{amb}$, but also other forms of energy dissipation: residual heat dissipation stream $\dot{Q}_r$, which is a measure of energy losses not included in the energy balance (e.g. the stream of acoustic energy and mechanical vibration from the thermal-fluid and mechanical systems of the entire power unit) [7]. Formula (1) shows the relationship that allows the engine energy balance to be drawn up:

$$\dot{Q}_{fuel} + \dot{H}_{air} = \dot{H}_{exh} + \dot{Q}_{oil} + \dot{Q}_{cool} + \dot{Q}_{amb} + \dot{Q}_r + P_i \quad (1)$$

The thermal efficiency of the engine η_{th} is expressed as the ratio of the average indicated power P_i to the energy supplied to the engine (2):

$$\eta_{th} = \frac{P_i}{\dot{Q}_{fuel} + \dot{H}_{air}} \quad (2)$$

Visualization makes it possible to identify potential faults in functional systems. It also ensures the creation of a clear energy balance, assigning all input energy to useful work and its distribution to losses occurring in each engine's functional system. The measured data is used in the energy balance equations and then presented graphically in a Sankey diagram [1].

3. Obtained results of simulations and research

3.1. Numerical simulation in the Blitz-PRO program

The issues presented in this section were focused on the numerical analysis of thermodynamic processes occurring in an appropriately modeled Andoria S320 four-stroke, single-cylinder diesel engine.

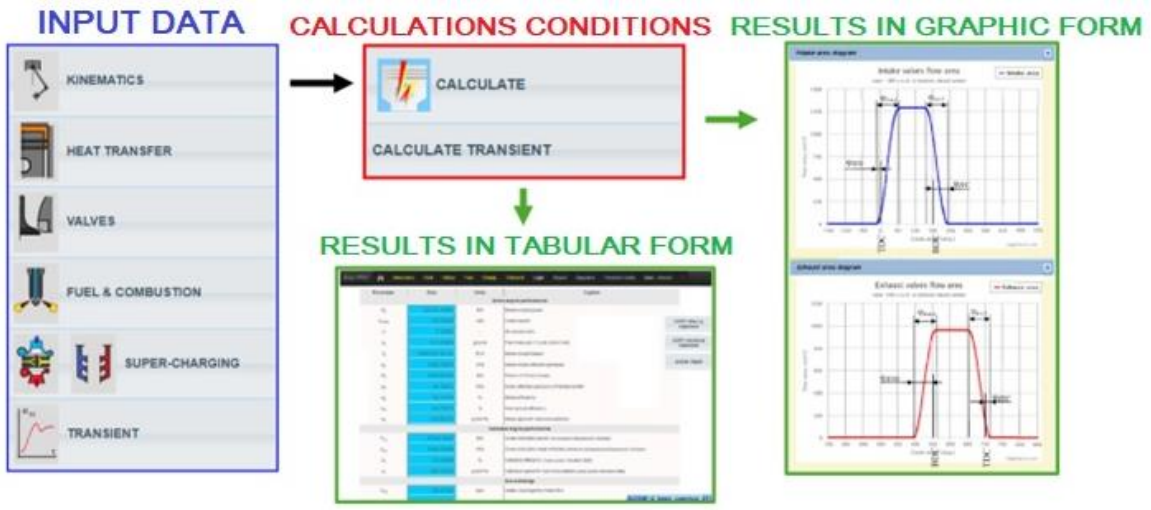

Fig. 1. Schematic of project management in Blitz-PRO software [2]

Numerical simulations in Blitz-PRO software were carried out in the first place, so it was possible to obtain results in a fast and non-invasive way. Based on the analysis of the simulation results, an assessment was made as to whether the implemented damage caused the expected effects, in the form of sufficiently noticeable changes in the values of parameters that could be recorded on the test bench. The second objective of the simulations carried out was to assess the correctness (validation) of the numerical tool's performance against the results of the tests carried out on the test bench.

Blitz-PRO simulation software makes it possible to analyze the thermodynamic cycle of internal combustion engines, including four-stroke IC engines. For each engine configuration, the basic approach remains the same: a division of the engine into several thermodynamic systems is made, interacting with each other through energy and mass exchange processes. The results of numerical simulations are compiled both in the form of a so-called report and diagrams representing the processes occurring during operation of the modeled engine [2,17].

Figure 1 presents a simplified form of the scheme for solving numerical simulations, taking into account the most important stages of project management.

According to the data shown in Fig. 1, proceeding to conduct numerical simulations must be preceded by the modeling of the engine under study, which involves implementing all the necessary parameters in such a way as to reproduce the structural and physical quantities of the various functional systems with the greatest possible precision [2].

The "Kinematics" tab allows configuration of the main geometric properties of the engine, i.e. cylinder diameter, piston stroke, number of cylinders and geometric compression ratio.

In the next section, the "Heat transfer" tab referring to frictional losses and heat transfer from the intake manifold, exhaust manifold and heat transferred due to piston motion to the boundary walls of the intra-cylinder space should be configured accordingly.

The next section, "Valves," refers to the valve components responsible for charge exchange in the combustion chamber. It mainly contains the geometric design parameters of the valve system, as well as the positions and durations of valve opening and closing [°CA].

The "Fuel & Combustion" section deals with the configuration of parameters related to the fuel injection system. It includes both information about the design of the injector and the characteristics of the fuel used.

The "Super-Charging" engine gas exchange system includes the selection of the configuration and geometric properties of the intake system and exhaust manifold, the method of cylinder charging, the type and number of compressors and their arrangement. It is possible to carry out calculations for a naturally aspirated engine (laboratory bench case) and supercharged engines.

With reference to the research objective of evaluating the effectiveness of using Sankey diagrams for diagnostics, a necessary step was to correctly model the engine located on the test bench. This was done by implementing the correct values in each of the described tabs.

Numerical simulations were carried out for three engine operating states. The reference state of the engine, which did not include any malfunction, was taken as the reference point for the analyses. The second state included a malfunction related to the engine's air intake system, while the third state was directly related to the fuel injection system into the combustion chamber. For all numerical operations, one engine operating point was selected for which the average value of fuel injection pressure was equal to the rated value of this parameter for the Andoria S320 engine $(p_{inj} = 14\ \mathrm{MPa})$. Simulations were carried out for an effective power, equal to $P_e = 10.8\ \mathrm{kW}$ $(0.82 \cdot P_N)$ and a crankshaft speed of 1200 min^{-1}. Analyses conducted for smaller loads indicated similar relationships to those whose results are presented in this article. The calorific value of the fuel used in the simulations was 42.5 MJ/kg. The temperature of the fuel was the same as the ambient temperature. Ambient conditions: t_{amb} = 20°C, p_{amb} = 101.3 kPa, humidity 30%. Coolant temperatures were: at the inlet to the cylinder liner 358 K, at the inlet to the piston 368 K, at the inlet to the cylinder head 358 K. Intake valve opening was 23°CA

before TDC, closing was 40°CA after BDC. Exhaust valve opening was 46°CA before BDC, closing was 17°CA after TDC. The injection advance angle was 32°CA before TDC, while the injection duration was 28°CA.

The output from the simulations made it possible to draw up energy balances for each engine operating condition, and consequently to graphically form them in the form of Sankey diagrams.

The first of the two faults implemented was to simulate fouling of the air filter feeding the cylinder section. The introduction of the malfunction into the intake system was done via changes made to the input parameters of the numerical simulator. For the reference condition, the internal area of the intake manifold was $A_{in} = 0.0035\ m^2$. In the case currently under consideration, this area was reduced by 80%, so this parameter was set at $A_{in} = 0.0007\ m^2$. The reduction in cross-sectional diameter also prompted a change in the value of pressure drop in the intake duct from $\Delta p_{in} = 1$ kPa (the value for the reference condition), to $\Delta p_{in} = 8$ kPa.

The second case of implemented failure represents a malfunction in the fuel injection system. This malfunction is directly related to the incorrect nature of the injector, so a component that, according to statistics in the literature, accounts for as much as 41% of all defects in the fuel supply system of diesel engines [3]. The malfunction in this system was implemented via changes in such parameters as the free-flight distance of the fuel jet and droplet diameters, for example. The result of such an action was, in effect, a reduction in the average fuel injection pressure p_{inj} by about 10% relative to the reference condition.

Table 1 summarizes the values of the component parameters of the energy balances, determined by numerical simulations. The green and red colors also indicate, in turn, the percentage increase or decrease in values relative to the reference condition. The data in Table 1 were also used to reflect the balances in graphical form, using Sankey diagrams, illustrated in Fig. 2.

For each of the analyzed cases, the highest loss in the balance was recorded in the form of heat flow absorbed by the engine cooling water $\dot{Q}_{cool}$, with the values of this parameter varying in magnitude. The throttling of the air intake contributed to an increase in the generated loss by 14.44%, while in the case of the second failure, the value decreased by 15.4% relative to the reference. The malfunction of the fuel supply system significantly reduced the loss associated with the heat flux absorbed by the engine oil, $\dot{Q}_{oil}$, by 17.27% relative to the condition representing a fully operational engine. The total value of the heat flux raised from the external surfaces of the engine to the environment by radiation and the flux of the rest of the heat dissipated $(\dot{Q}_{amb} + \dot{Q}_r)$ is the resulting value of the balance – the reports do not take these parameters into account.

In the great majority of the balance's component parameters, deviations from the reference values are within the limits of calculation error. The balances supplemented by the efficiencies (thermal η_{th}, mechanical η_m and overall η_o) showed that the reference condition in the overall comparison presented the worst, with the highest overall efficiency of the engine obtained for the condition taking into account the inefficiency of the fuel supply system: 25.91% (a 5.23% increase over the reference condition).

Reducing the cross-sectional area of the intake air duct by 80% resulted in about a 12% reduction in the heat delivered with the fuel. This is believed to be caused by a multiplicity of phenomena occurring simultaneously: throttling the airflow results in an increase in flow velocity, and consequently, losses of many types increase. In addition, the heat flow depends on the mass flow rate of the air flowing through. In turn, the mass flux depends on the cross-sectional area of the duct (which decreases) and the flow velocity (which increases). Less air always results in worse combustion conditions.

In the case of a noticeable increase in the enthalpy flux of the exhaust gas with a reduced injector opening pressure, it can be assumed that worse fuel atomization results in a decrease in the duration of combustion, and thus an increase in the temperature of the exhaust gas, which directly affects the enthalpy value. Reduced injector opening pressure always results in worse atomization and penetration of fuel particles in the combustion chamber.

Table 1. Components of the energy balance of the Andoria S320 engine (numerical simulations)

		Reference condition	Throttled air intake		Reduced injection pressure	
Parameter	Unit	Value	Value	δ_{REF} [%]	Parameter	Unit
$\dot{Q}_{fuel}$	[kW]	37.093	38.755	4.480	34.976	5.707
$\dot{H}_{air}$	[kW]	5.074	4.468	11.949	5.130	1.102
$\dot{H}_{exh}$	[kW]	7.425	7.082	4.619	7.629	2.746
$\dot{Q}_{cool}$	[kW]	11.714	13.406	14.440	9.910	15.403
$\dot{Q}_{oil}$	[kW]	4.128	4.258	3.151	3.415	17.270
$\dot{Q}_{amb} + \dot{Q}_r$	[kW]	5.125	4.726	7.774	5.531	7.937
P_i	[kW]	13.776	13.751	0.180	13.621	1.122
P_m	[kW]	2.998	2.939	1.982	2.822	5.862
P_e	[kW]	10.778	10.812	0.321	10.799	0.197
η_{th}	[%]	32.670	31.815	2.618	33.964	3.960
η_m	[%]	75.360	75.060	0.399	76.283	1.225
η_o	[%]	24.620	23.880	3.006	25.909	5.233

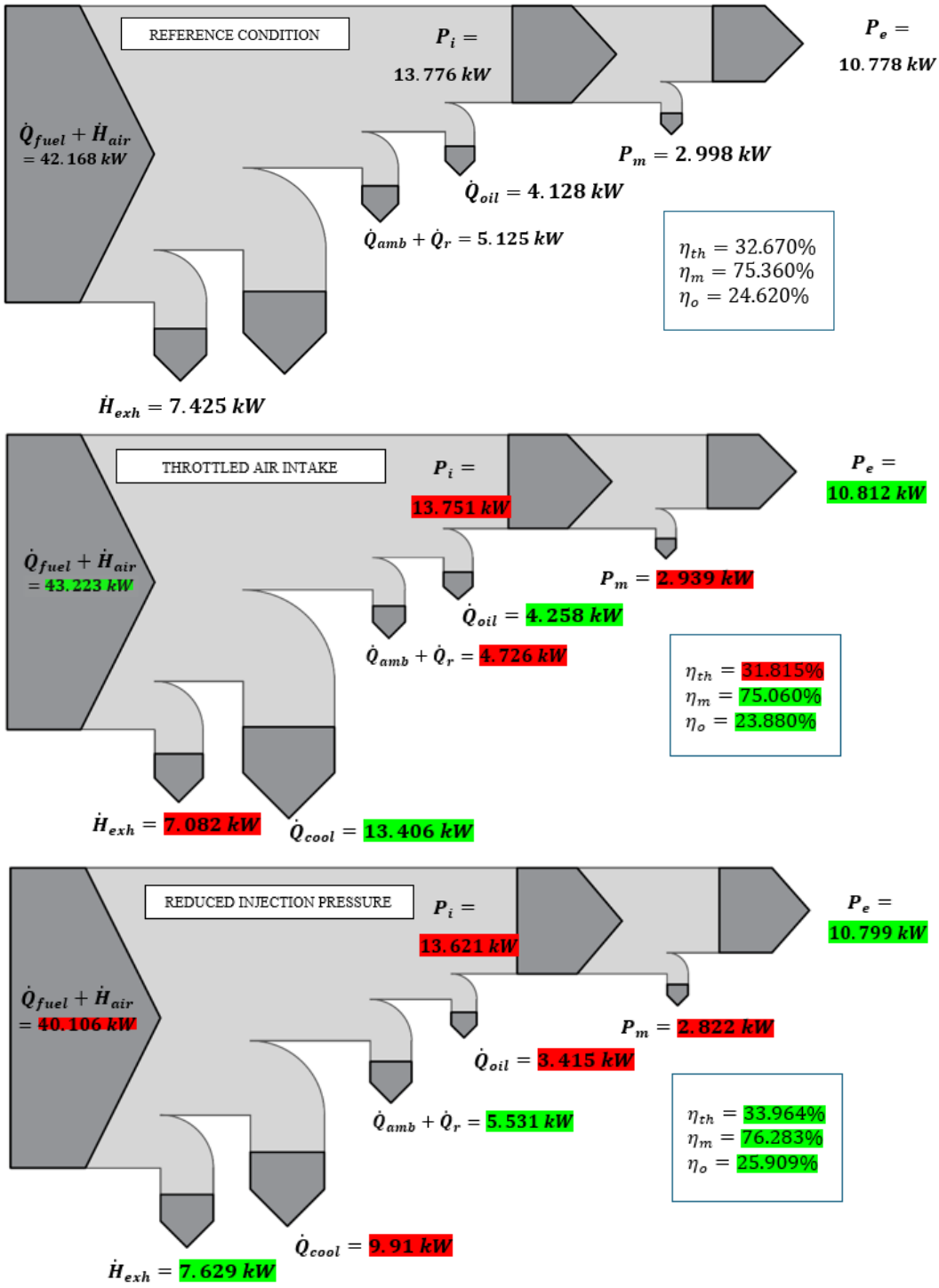

Fig. 2. Sankey diagrams – results of numerical simulations

The increase in the amount of heat received by the coolant and lubricating oil in the case of throttled air can be interpreted as a result of less oxygen in the combustion chamber, and thus an increase in the temperature of the circuit and an increase in the intensity of heat transfer.

With the changes introduced in the simulations, we are dealing with very complicated thermodynamic and flow phenomena. The mathematical algorithm of the software used is not fully known to the user, but it is treated as correct because of the publication support [9, 17].

3.2. Measurement results on the laboratory bench

The measurements were carried out on a test stand located in the Mechanical Engineering Laboratory of the Faculty of Mechanical Engineering and Ship Technology of Gdansk University of Technology. A single-cylinder, four-stroke IC engine powered by diesel fuel – Andoria S320 – was used (Fig. 3 and 4). The engine under study is characterized by a maximum power of 13.2 kW at a crankshaft speed of ,500 min^{-1} and a maximum torque of 84.4 Nm at 1200 min^{-1}. A summary of the most important values of the engine's technical parameters is presented in Table 2.

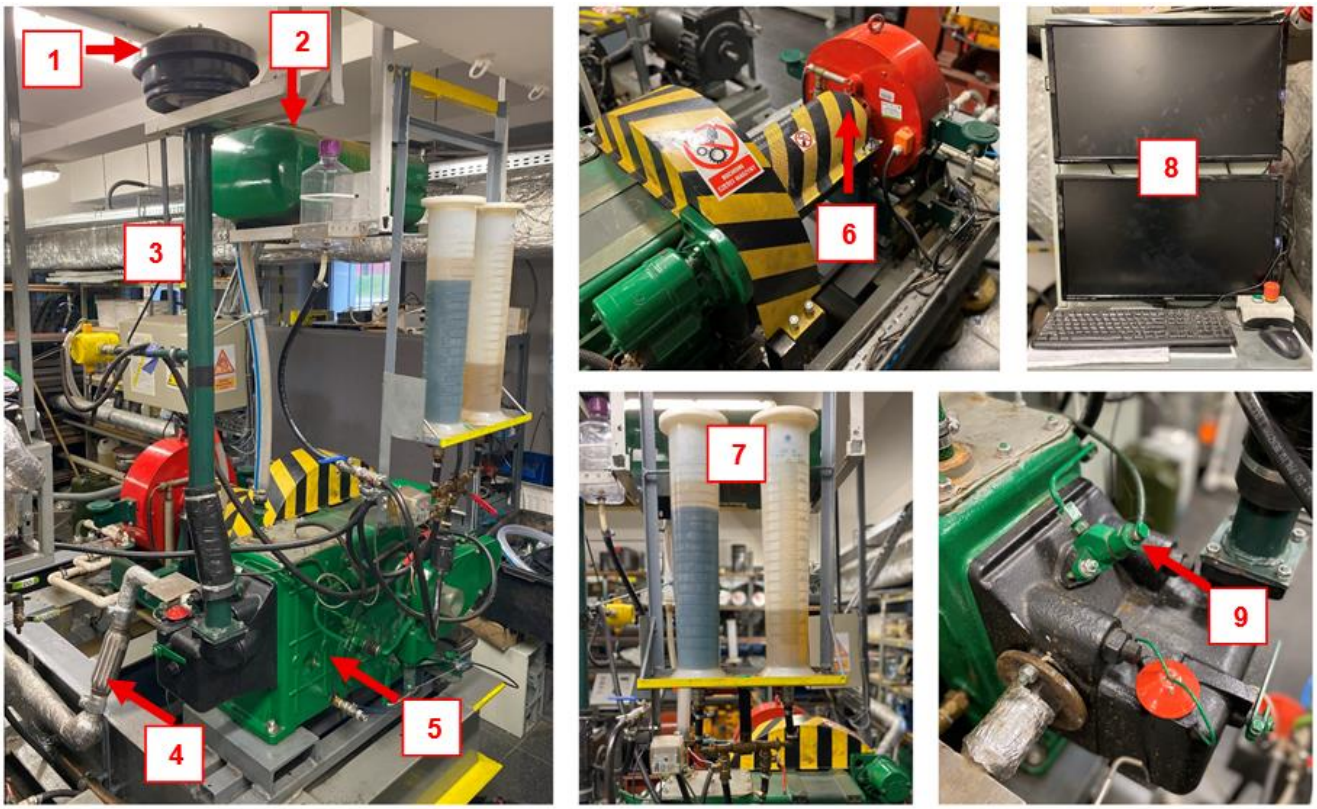

Fig. 3. Andoria S320 diesel engine test stand: 1 – air filter, 2 – engine cooling water tank, 3 – intake air duct, 4 – exhaust gas duct, 5 – Andoria S320 engine, 6 – water-cooled brake, 7 – supply fuel tanks, 8 – control and measurement software cabinet, 9 – injector

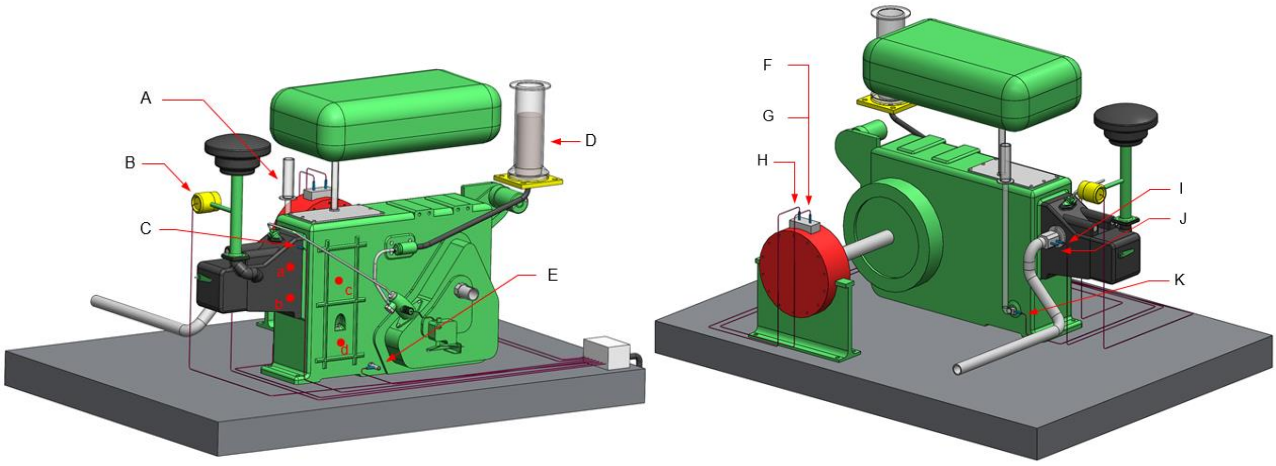

Fig. 4. Model of the test bench – front and back parts: A – cooling water level indicator, B – air flow rate meter, C –points for measuring the temperature of the surface of the engine, D – fuel level indicator, E –lubricating oil temperature measurement point, F – crankshaft rotational speed measurement, G – torque measurement, H – water-cooled brake, I – exhaust gas temperature measurement point, J – exhaust gas analyzer mounting point, K – cooling water temperature measurement

Table 2. Technical data of Andoria S320 engine

Parameter	Value	Unit
Displacement volume	1810	cm^3
Cylinder diameter	120	mm
Piston stroke	160	mm
Compression ratio	17	–
Injection advance angle	32	°CA
Injection pressure	17	MPa

Computer software provides both a live reading of sensor readings and smooth control of engine crankshaft speed and torque. The drive shaft is connected to a water-cooled brake, making it possible to conduct tests for preset engine loads.

Optrand D32294-Q sensor was used to measure the indicated software, it was possible to indicate the temperatures at the adopted measurement points and then calculate the $\dot{Q}_{amb}$ [14, 16].

Tests on the test bench were carried out in a similar manner to numerical simulations (three technical condi-

tions). Regardless of the analyzed operating state, all measurements were made for a strictly defined crankshaft speed setting of 1200 min^{-1} and a torque of 40 Nm, consequently, the tests were carried out for an engine load equal to 38% of rated power. Malfunctions introduced into the intake air system were accomplished by restricting the flow area through the filter in such a way as to reduce the flow by about 50%. The impairment to the fuel supply system was introduced by means of a reduction in fuel injection pressure. This parameter was reduced from a reference value of 17 MPa to a value of 15 MPa, therefore by 12%.

During the laboratory test, the opening and closing angles of the intake and exhaust valves were the same as in the simulation. The same was the case with the injection timing advance angle. Water was cooling the engine by evaporation at 100°C. The tests were conducted at a lubricating oil temperature of 45°C. Summer diesel oil was used, the fuel temperature was the same as the ambient temperature. The ambient conditions were t_{amb} = 15°C, p_{amb} = 100.6 kPa, humidity 50%.

Table 3 presents the energy balances, in the form of energy input totals and energy losses, for each engine operating condition analyzed. Finally, Sankey diagrams for each engine operating condition are shown in Fig. 5.

By subjecting the presented Sankey diagrams (Fig. 5) to analysis for the three operating states of the Andoria S320 engine, it was found that there were no significant differences in the values of the heat balance components. The results obtained suggest a minimal effect of implemented damage on the efficiency of engine operation.

In the reference condition, which is the reference point for the analyses carried out, the input energy to the engine $(\dot{Q}_{fuel} + \dot{H}_{air})$ amounted to 21.468 kW, with the largest losses falling on the exhaust enthalpy stream $(\dot{H}_{exh} = 9.943\ kW)$, while accounting for 46% of the total energy supplied to the engine. Obtained from thermal imaging camera measurements, the value of heat flow radiated from the engine's external surfaces to the environment was $\dot{Q}_{amb} = 1.760\ kW$. In the context of the analysis of the components of the heat balance, it is reasonable to note the almost negligibly small value of the heat flow taken up by the water in the coolant expansion tank $\dot{Q}_{cool}$, equal to 0.054 kW. For each of the other two engine operating states, values of the same order of magnitude were obtained. It is presumed that the obtained results related to this parameter, may be subject to some measurement error, resulting from the analog form of the reading.

Thus, significant differences were observed in the values of the results with respect to the results of numerical simulations, for which the heat flow extracted by water, in turn, was characterized by the dominant magnitude among all heat loss streams considered. The inconsistency of the values obtained through testing can also be confirmed by literature data, indicating that the average value of engine cooling losses is 26% [18]. Other component quantities of the energy balance obtained by numerical simulations also showed a significant deviation from the results of bench tests. Despite the noticeable differences for the two chosen paths (simulation and measurement), similar values of the overall efficiency of the engine η_o, were registered, with the numerical software taking the parameter to higher values, regardless of the engine's operating condition. In general, however, it should be borne in mind that the engine modeled in the Blitz-PRO numerical software represented values for a "new" engine, which in turn was not possible to verify the test object on the test bench.

Further analyzing the results obtained from the measurements, the component $\dot{Q}_r$, which is the residual heat dissipation stream (the stream of acoustic energy and mechanical vibration of the entire power unit), was juxtaposed as a summed value with the heat flow absorbed by the oil $\dot{Q}_{oil}$. This approach was used because the stream of residual heat dissipated is a measure of energy losses not included in the heat balance [7]. Then, for the reference condition, the value obtained was $\dot{Q}_{oil} + \dot{Q}_r = 1.527\ kW$. The value of the indicated power was $P_i = 8.104\ kW$, while the effective power was $P_e = 5.074\ kW$, with thermal efficiency $\eta_{th} = 37.748\ \%$, mechanical efficiency $\eta_m = 62.612\ \%$ and overall efficiency $\eta_o = 23.634\ \%$.

Table 3. Components of the energy balance of the Andoria S320 engine (test results)

		Reference condition	Throttled air intake		Reduced injection pressure	
Parameter	Unit	Value	Value	δ_{REF} [%]	Value	δ_{REF} [%]
$\dot{Q}_{fuel}$	[kW]	16.366	15.969	2.429	15.942	2.591
$\dot{H}_{air}$	[kW]	5.101	5.208	2.097	5.159	1.135
$\dot{H}_{exh}$	[kW]	9.943	9.971	0.290	9.825	1.179
$\dot{Q}_{cool}$	[kW]	0.054	0.046	14.865	0.057	5.405
$\dot{Q}_{amb}$	[kW]	1.760	1.764	0.255	1.784	1.368
$\dot{Q}_{oil} + \dot{Q}_r$	[kW]	1.608	1.527	5.049	1.230	23.492
P_i	[kW]	8.104	7.869	2.897	8.205	1.257
P_m	[kW]	3.030	2.836	6.381	3.147	3.853
P_e	[kW]	5.074	5.032	0.817	5.059	0.293
η_{th}	[%]	37.748	37.157	1.565	38.855	3.014
η_m	[%]	62.612	63.953	2.142	61.653	1.531
η_o	[%]	23.634	23.763	0.544	23.974	1.437

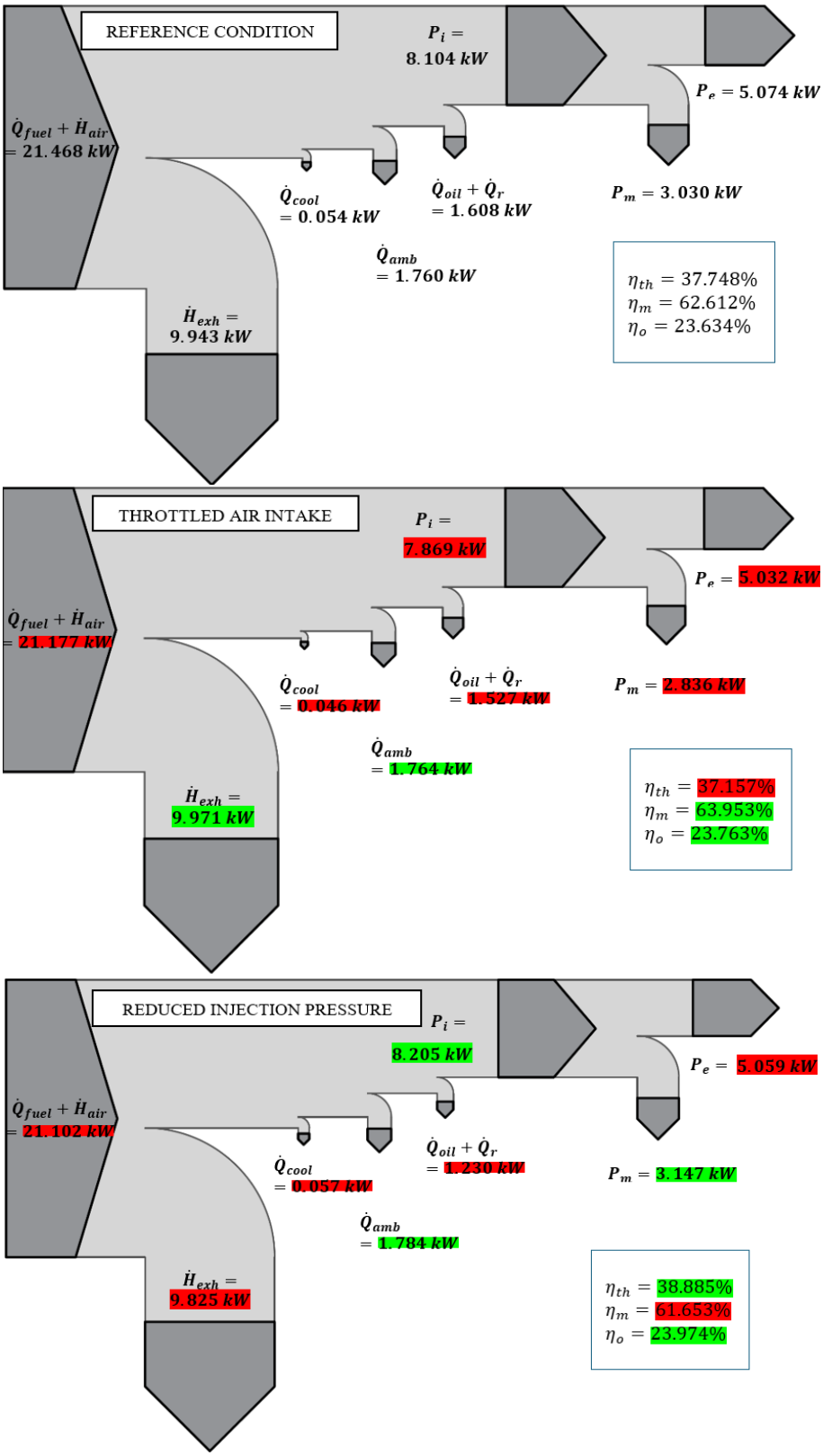

Fig. 5. Sankey diagrams – laboratory results

When the airflow through the filter was reduced by 50%, there was a slight deviation from the reference condition. The input power stream decreased slightly to a value of 21.177 kW (a decrease of 1.35%), indicating a minimal effect of this type of implemented damage on the considered parameter. There was also a 2.9% decrease in induced power P_i from 8.104 kW to 7.869 kW. The consequence of this was also a decrease in the thermal efficiency of the engine η_{th}. Since the mechanical loss power decreased from the reference condition by 6.38%, the overall benefit was observed with a minimal increase in mechanical efficiency η_m, equal to 2.14% (η_m = 63.953 %).

For the condition with reduced fuel injection pressure (17 MPa → 15 MPa), no significant changes were observed in the values of the components of the engine heat balance parameters. The largest deviation from the reference value (as much as 23.5%) was obtained for the heat flow extracted by oil $\dot{Q}_{oil}$, but since this is the resulting value of the other components, it proves difficult to adequately justify the possible reason for such a deviation. As a result of the small changes (relative to the reference condition) in the losses in the form of heat streams, the thermal, mechanical, and overall efficiencies also did not change significantly. Nevertheless, the overall efficiency η_o increased by 1.44% relative to the condition characterized by normal engine operation.

One of the reasons for the discrepancies in the results obtained by simulation and during laboratory testing may be different engine cooling conditions. While the simulation assumes the flow of coolant through the engine, the laboratory bench considers cooling by evaporation of water in the cooling tank. This and several smaller differences between the engine implemented in the program and that on the test bench can result in differences when validating both results.

4. Conclusions

Summarizing the research, calculations, and analyses carried out, the following conclusions were drawn:

– The assumption of carrying out numerical simulations was fulfilled, as changes were recorded in those values of the heat balance components that could be associated with the damage introduced into the model.

– Conducting tests under an engine load equal to 38% of rated power, was in line with the stated goal of verifying that, in a situation where testing at operating load is not possible, the engine's functional systems provide a diagnostic signal in the form of changes in the components of the energy balance. The results obtained confirmed consistency with existing literature conclusions, indicating that low-load tests are unable to provide a satisfactory result.

– It was shown that, regardless of the fault implemented, in the case of both the intake air system and the fuel supply system malfunctions, none of the balance components showed significant deviations from the reference condition. Variations of 2–3% are below the standard statistical error, caused, among other things, by the measurement accuracy of the instruments used, but also by the possibility of misreading analog readings.

– The following are considered to be the causes of incorrect (in relation to theoretical knowledge) increase/decrease in the value of the heat balance component: for simulations, inferior combustion conditions due to changes in the functional systems of the engine, for tests, insufficient water cooling. Different input data, such as technical condition, laboratory conditions, or a correct, but idealized calculation algorithm, are considered to be the reason for the lack of compatibility between the model and the tests.

– Engine load affects the way heat is released, as a higher fuel injection rate leads to faster injection and more intense combustion. An increase in injection speed causes the injection time to increase more slowly than the fuel dose, and combustion occurs more simultaneously. At a lower load, the auto-ignition delay lengthens, which reduces the maximum heat release rate in the initial phase of combustion. This phenomenon and others accompanying it simultaneously affect the various components of the engine's heat balance.

– On the test bench, it was not feasible to evaluate the mechanical and thermal condition of the engine's functional systems, even for the reference case. It was also not possible to input the engine's technical condition into the Blitz-PRO simulator. This may have had some impact on the results.

– The results obtained suggest continuing work on the development of the numerical software used, given its high potential.

Nomenclature

BDC	bottom dead center
$\dot{H}_{air}$	air enthalpy stream
$\dot{H}_{exh}$	exhaust gas enthalpy stream
IC	internal combustion
p_{amb}	ambient air pressure
P_e	effective power
P_i	indicted power
P_m	mechanical power
P_N	nominal power
$\dot{Q}_{amb}$	ambient heat stream
$\dot{Q}_{cool}$	cooling heat stream
$\dot{Q}_{fuel}$	fuel heat stream
$\dot{Q}_{oil}$	oil heat stream
$\dot{Q}_r$	residual heat stream
t_{amb}	ambient air temperature
TDC	top dead center
δ_{REF}	difference from the reference condition
η_m	mechanical efficiency
η_o	overall efficiency
η_{th}	thermal efficiency

Bibliography

[1] Baldi F, Gabrielli C, Andersson K. From energy flows to monetary flows – an innovative way of assessing ship performances through thermo-economic analysis. 2012. https://publications.lib.chalmers.se/records/fulltext/159874/local_159874.pdf

[2] Blitz-PRO Software Manual (accessed on 12.11.2024). http://blitzpro.zeddmalam.com/application/index/about

[3] Bocheński C, Janiszewski T. Diagnostyka silników wysokoprężnych (Diesel engine diagnostics). Wydawnictwo Komunikacji i Łączności. Warszawa 1996.

[4] Duda K, Wierzbicki S, Mikulski M. An experimental analysis of performance and exhaust emissions of a CRDI diesel engine operating on mixtures containing mineral and renewable components. Combustion Engines. 2019;179(4):27-31. https://doi.org/10.19206/CE-2019-404

[5] Jaichandar S, Samuelrai D, Sathish Kumar M. Effects of varying injector opening pressure on the performance of a B20 JOME biodiesel fueled engine. Journal of Mechanical Engineering. 2019;16(1). https://doi.org/10.24191/jmeche.v16i1.6031
[6] KIGAZ 310 Technical Specifications (accessed on 12.11. 2024). https://www.metris.pl/produkt/kimo-kigaz-310-analizator-spalin-z-sond-z-wymiennymi-czujnikami/
[7] Korczewski Z. Metodyka testowania paliw żeglugowych w rzeczywistych warunkach pracy silnika o zapłonie samoczynnym (Methodology for testing marine fuels under real compression ignition engine operating conditions). Wydawnictwo Politechniki Gdańskiej. Gdańsk 2022.
[8] Korczewski Z. Thermal efficiency investigations on the self-ignition test engine fed with marine low sulfur diesel fuels. Combustion Engines. 2019;178(3):15-19. https://doi.org/10.19206/CE-2019-303
[9] Minchev D, Gogorenko O. Effect of thermal inertia on diesel engines transient performance. Internal Combustion Engines. 2020;1:68-72. https://doi.org/10.20998/0419-8719.2020.1.09
[10] Optrand D32294-Q Technical Specifications (accessed on 12.11.2024). https://www.optrand.com/apsis.htm
[11] Paszota Z. Losses and energy efficiency of drive motors and systems. Polish Maritime Research. 2013;20(1):3-10. https://doi.org/10.2478/pomr-2013-0001
[12] Puzdrowska P. Diagnosis of marine internal combustion engines by means of rapidly variable temperature and composition of exhaust gas as an alternative or support for currently used diagnostic methods. Combustion Engines. 2025; 200(1):19-30. https://doi.org/10.19206/CE-193951
[13] Skobyłko J. Analiza możliwości wykorzystania w diagnostyce silnika o ZS wykresu Sankey'a (Analysis of the possibility of using Sankey diagram in the diagnostics of the diesel engine) Master's thesis. Gdańsk University of Technology. Gdańsk 2025.
[14] Software specification InfReC Analyzer NS9500LT (accessed on 12.11.2024). https://www.infrared.avio.co.jp/en/support/thermo/download/ns9500lt-dl/
[15] Sroka ZJ, Prakash S, Wlostowski R. Design of the turbocharger bearing arrangement to increase the overall efficiency of the combustion engine. Combustion Engines. 2022; 188(1):83-89. https://doi.org/10.19206/CE-142348
[16] Technical specifications of NEC Thermo Gear G30 thermal imaging camera (accessed on 12.11.2024). https://www.infrared.avio.co.jp/en/products/ir-thermo/lineup/g30/index.html
[17] Varbanets R, Minchev D, Kucherenko Y, Zalozh V, Kyrylash O, Tarasenko T. Methods of real-time parametric diagnostics for marine diesel engines. Polish Maritime Research. 2024;31(3):71-84. https://doi.org/10.2478/pomr-2024-0037
[18] Włodarski JK, Witkowski K. Okrętowe silniki spalinowe. Podstawy teoretyczne. (Ship internal combustion engines. Theoretical fundamentals). Wydawnictwo Akademii Morskiej w Gdyni. Gdynia 2006.

Patrycja Puzdrowska, DEng. – Faculty of Mechanical Engineering and Ship Technology, Gdańsk University of Technology, Poland.
e-mail: *patpuzdr@pg.edu.pl*

Jakub Skobyłko, Eng. – Faculty of Mechanical Engineering and Ship Technology, Gdańsk University of Technology, Poland.
e-mail: *s182565@student.pg.edu.pl*